1922—2022

Petrogenesis of the Early Jurassic Longtang and Menglong Peraluminous Granites in Tengchong Terrane, and their Tectonic Implication

WANG Guochang[1], LIU Zheng[2,*], TAN Shucheng[2], HE Xiaohu[2], WANG Yuchao[2], QI Changshi[1] and YE Hui[3]

[1] *Institute of Palaeontology, Yunnan Key Laboratory for Palaeobiology, MEC International Joint Laboratory for Palaeobiology and Palaeoenvironment, Yunnan University, Kunming 650500, China*
[2] *School of Earth Science, Yunnan University, Kunming 650500, China*
[3] *Institute of International Rivers and Eco-security, Yunnan University, Kunming 650500, China*

Abstract: A comprehensive study of zircon U-Pb geochronology, in situ Hf isotopes, whole-rock major and trace element geochemistry, and Nd isotopes was carried out for two Early Jurassic two-mica granites (Longtang and Menglong) in the southern part of the Tengchong terrane, which is in the northern part of the larger Sibumasu terrane. We assess the origin of the granites and explore their possible genetic relationship to the Paleo-Tethyan regime. LA-ICP-MS zircon U-Pb dating shows that they were simultaneously emplaced in the Early Jurassic (ca. 199 Ma). They have SiO_2 contents of 69.7–75.1 wt% and are mainly strongly peraluminous with alumina saturation index (ASI) values ranging from 1.06 to 1.46. They show similar $Mg^{\#}$ (0.29–0.42) to experimental partial melts of metasedimentary rocks under continental pressure-temperature (*P-T*) conditions. They are enriched in light rare earth elements (LREEs) relative to heavy rare earth elements (HREEs), with moderately negative Eu anomalies and flat HREEs patterns. They show negative $\varepsilon_{\mathrm{Nd}}(t)$ values (−9.0 to –12.4) and $\varepsilon_{\mathrm{Hf}}(t)$ values (−8.0 to −9.1). Elemental and isotopic data suggest that they most likely to formed by muscovite-dehydration melting of a metapelitic source at lower temperatures in the range of 700°C to 750°C. The granites might represent a post-collisional tectonic setting response to Paleo-Tethyan regime.

Key words: peraluminous granites, post-collision, Early Jurassic, Paleo-Tethys, Tengchong terrane

Citation: Wang et al., 2022. Petrogenesis of the Early Jurassic Longtang and Menglong Peraluminous Granites in Tengchong Terrane, and their Tectonic Implication. Acta Geologica Sinica (English Edition), 96(6): 1979–1990. DOI: 10.1111/1755-6724.14925

1 Introduction

The Sibumasu terrane, including the Baoshan and Tengchong terranes in southwest China, separated from the northwest margin of Gondwana in the late Early Permian and finally collided with the Simao-Indochina terrane after the closure of the Paleo-Tethys Ocean and the Sukhothai back-arc ocean (Metcalfe, 2013; Wang et al., 2018). However, the timing of the collision remains controversial, with suggestions ranging from the Late Permian (Feng et al., 2002), to the Early to Mid-Triassic (Hennig et al., 2009), and even the Late Triassic (Searle et al., 2012; Metcalfe, 2013; Cai et al., 2017; Wang et al., 2018). Granitoids, as products of re-melted continental crust, are usually employed as an ideal geological tracer to explore crustal tectonic evolution (Pearce, 1996; Pitcher, 1997). The Triassic to earliest Jurassic granitoids in the Tengchong terrane of northern Sibumasu terrane were suggested to be the magmatic products of either an arc, syn-collisional, or post collisional tectonic setting related to the East Paleo-Tethys Ocean, or even an arc tectonic setting related to the Meso-Tethys Ocean (Cong et al., 2010; Zou et al., 2011; Huang et al., 2013; Wang et al., 2018; Zhu et al., 2018; Cao et al., 2019).

In this paper, we present detailed LA-ICP-MS zircon U-Pb geochronology, in situ Hf isotope, whole-rock major and trace element geochemical, and Nd isotope data for two Early Jurassic (ca. 199 Ma) two-mica granites (Longtang and Menglong) of southern part of the Tengchong terrane (Figs. 1b, 2). We aim to assess their origin and explore their possible tectonic setting. Detailed elemental and isotopic compositions indicate that these two-mica granites are likely to have been formed by muscovite-dehydration melting of a metapelitic source at lower temperatures in the range of 700°C to 750°C at a normal crustal depth. Their emplacement might be associated with the post-collisional process between the Sibumasu terrane and the Simao-Indochina terrane after the final closure of East Paleo-Tethys Ocean.

2 Geological Setting

Mainland southeast Asia is a heterogeneous tectonic collage of continental crustal blocks, volcanic arcs, and suture zones that represent the remnants of closed oceans and back-arc basins (Metcalfe, 2011a, b, 2013; Metcalfe et al., 2017; Fig. 1a). The core area of mainland southeast Asia consists of, from west to east, the Sibumasu terrane, the Changning–Menglian, Chiang Mai–Chiang Rai, and

* Corresponding author. E-mail: liuzheng.0311@163.com

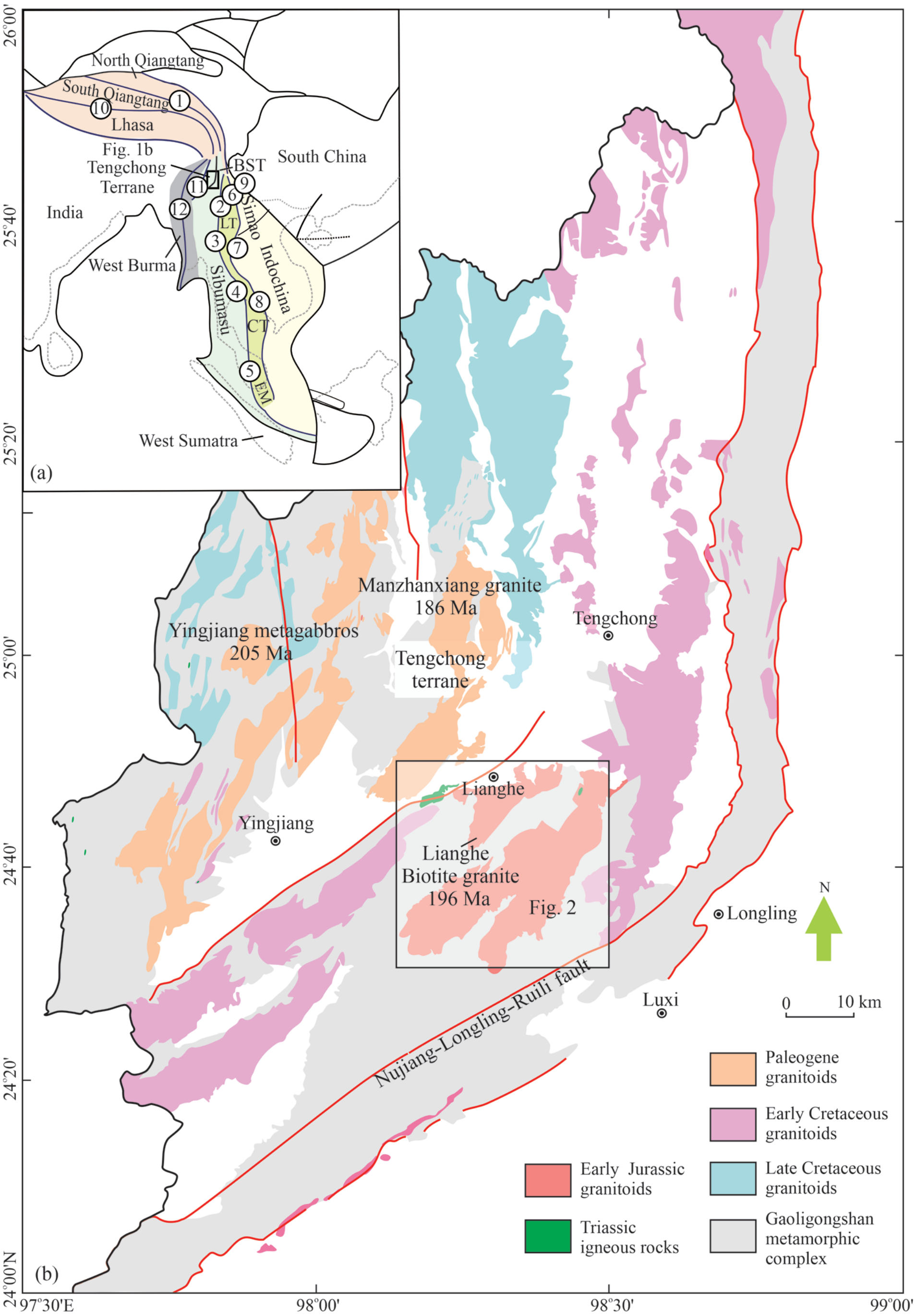

Fig. 1 (a) Simplified tectonic map of the eastern Tethyan tectonic domain and the location of the Tengchong terrane (after Metcalfe, 2013); (b) schematic regional geological map of the Tengchong terrane (after BGMRY, 1983; Cao et al., 2019).
In (a), also shown are arc terranes and sutures of eastern Asia. LT = Lincang arc terrane; CT = Chanthaburi arc terrane; EM = East Malaya; BST = Baoshan terrane; 1–Longmu Co Shuanghu; 2–Changning-Menglian; 3–Chiang Mai-Chiang Rai; 4–Chanthaburi; 5–Bentong-Raub; 6–Jinghong; 7–Nan-Uttaradit; 8–Sra Kaeo; 9–Ailaoshan; 10–Bangong; 11–Myitkyina; 12–Kalaymyo; In (b), also shown are Yingjiang metagabbros and Lianghe biotite granite (Zhu et al., 2018), Manzhanxiang granite (Cao et al., 2019).

Bentong–Raub suture zones, the Lincang–Sukhothai–East Malaya arc, the Jinghong–Nan–Sa Kaeo suture zones, and the Simao–Indochina terrane (Fig. 1a). The Changning–Menglian, Chiang Mai–Chiang Rai, and Bentong–Raub suture zones represent the remnants of the Paleo-Tethys Ocean, whereas the Jinghong–Nan–Sa Kaeo suture zones represent the remnants of the narrow and short lived Sukhothai back-arc ocean (Metcalfe, 2013).

The Tengchong terrane is located in the north of the Sibumasu terrane, southwestern Yunnan province, southwest China (Fig. 1a). It is fault-bounded by the Baoshan terrane along the Gaoligong dextral strike-slip fault to the east and the Ruili fault to the southeast, and by the West Burma terrane along the Sagaing fault to the

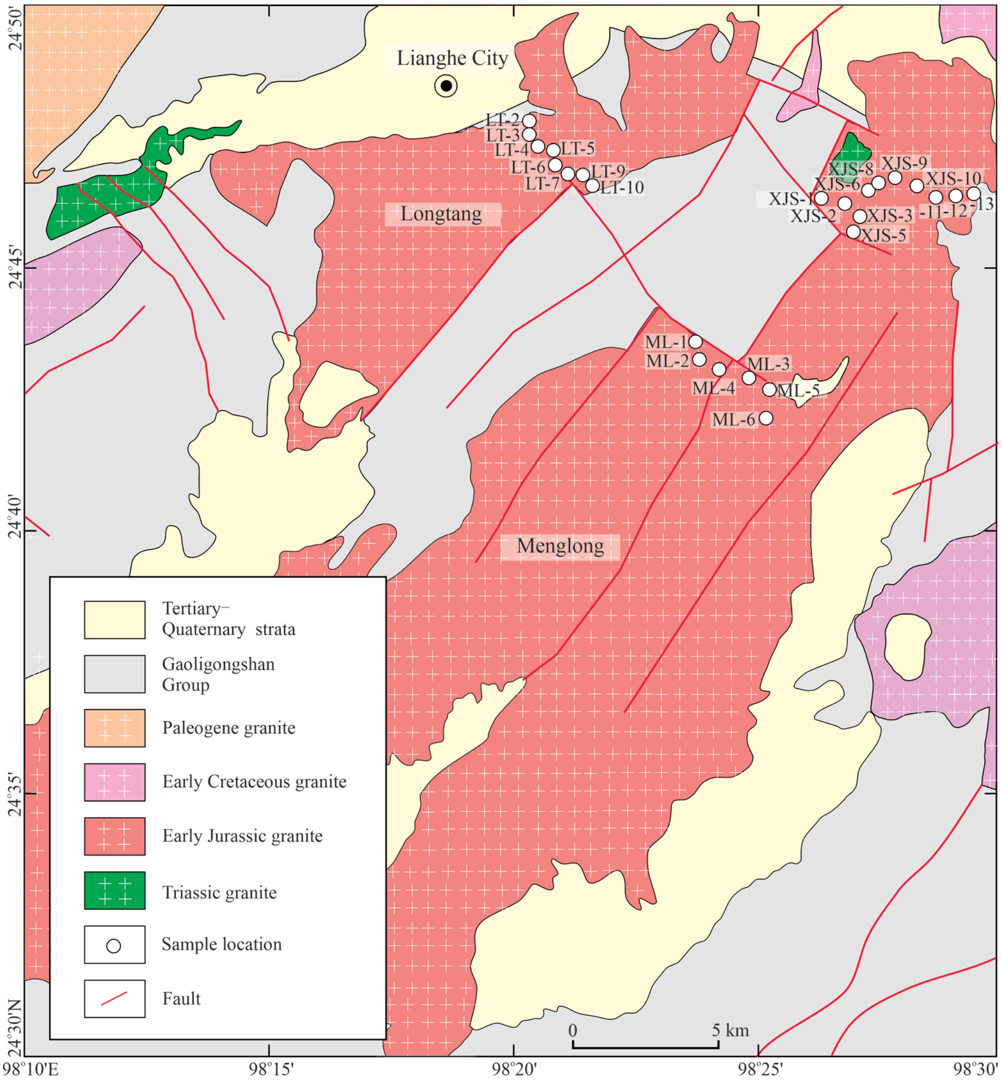

Fig. 2. Simplified geological map of the Longtang and Menglong granites in southern Tengchong terrane (after BGMRY, 1983).

west. The largest portion of the strata in the Tengchong terrane is occupied by the Gaoligongshan metamorphic complex (Fig. 1b), which is mainly comprised of high-grade pelitic gneiss, schist, migmatite and gneissic intrusions (Zhong, 1998; Li et al., 2016). The complex was previously regarded as Precambrian basement due to the high-grade metamorphism (generally to the amphibolite facies; Zhong, 1998). However, SHRIMP and LA-ICP-MS zircon U-Pb dating of the gneisses from the Gaoligongshan metamorphic complex in the Gongshan terrane indicate that they are metamorphosed Paleogene sediments that contain inherited Archean to Cretaceous detrital zircons (2690 Ma to 64 Ma) (Song et al., 2010). The overlying strata include lower Devonian to Lower Permian depositional sequences and Mesozoic clastic sedimentary rocks and carbonates. The Lower Devonian sequences contain siliciclastic rocks and dolomites and the Carboniferous to Lower Permian sequences consist of limestone, graywacke, pebble, pebble-bearing sandstones, and siltstones. Triassic sequences are exposed locally and they consist of shale, sandstone, and limestone. The Jurassic sequences also include shale, sandstone and limestone, whereas the Cretaceous sequences include siltstone, mudstone, and sandstone. Tertiary sandstone, siltstone, basaltic rocks, Quaternary conglomerate and sandstone are also exposed in the Tengchong terrane.

Extensive Mesozoic granitoids occur in the Tengchong terrane and can be divided into three major phases: Triassic (245–206 Ma) (Cong et al., 2010; Zou et al., 2011; Zhu et al., 2018), Early Cretaceous (140–110 Ma) (Cao et al., 2014, 2017, 2019; Zhu et al., 2015; Xie et al., 2016), and Late Cretaceous (80–65 Ma) (Chen et al., 2015; Cao et al., 2016, 2018, 2019). Recently, a few Early Jurassic granitoids were reported and their tectonic settings remain controversial (Zhu et al., 2018; Cao et al., 2019). The Longtang and Menglong granites intruded into the Gaoligongshan metamorphic complex at ca. 199 Ma (see below). Neither restites nor microgranular enclaves are observed. The granites consist of alkali-feldspar granite, syenogranite, and monzogranite. They consist of K-feldspar (30%–45%), plagioclase (10%–30%), quartz (30%–40%), muscovite (3%–5%), and biotite (3%–7%), with a medium-grained granitic texture (Fig. 3). The accessory minerals are sphene, apatite, and zircon. Some granites show minor alteration. The biotite was locally altered to chlorite, and the feldspars exhibit localized sericitization and argillation.

In this study, we collected twenty-five samples from surface exposures of the Longtang and Menglong granites. Sample locations are shown in Fig. 2. All samples were crushed to 200-mesh using an agate mill for whole-rock geochemical analysis. Two samples (LT-2, ML-4) were selected for LA-ICP-MS zircon U-Pb dating and in-situ zircon Hf isotope analysis. Zircons were separated using magnetic and heavy liquid separation methods, and then handpicked under a binocular microscope. Zircon grains were mounted in epoxy, and then polished for subsequent cathodoluminescence (CL) observation and LA-ICP-MS analysis.

3 Samples and Methods

3.1 LA-ICP-MS zircon U-Pb geochronology

Zircon U-Pb geochronology was conducted by LA-ICP-MS at Nanjing FocuMS Technology Co. Ltd. Both Australian Scientific Instruments RESOlution LR laser-ablation system (Canberra, Australian) and Agilent Technologies 7700x quadrupole ICP-MS (Hachioji, Tokyo, Japan) were combined for the experiments. The 193 nm ArF excimer laser was focused on zircon surfaces with a fluence of 3.5 J/cm^2. Each acquisition incorporated 20 s background (gas blank), followed by a spot diameter of 33 μm at a 5 Hz repetition rate for 40 s. Dwell times were set to 20 ms for ^{207}Pb, 15 ms for ^{206}Pb and ^{208}Pb, 10ms for ^{232}Th and ^{238}U, and 8ms for other trace elements. The external standard 91500 (1062 Ma) was employed to correct instrumental mass discrimination and elemental fractionation during the ablation (Wiedenbeck et al., 1995). GJ-1 (600 Ma) and Plešovice (337 Ma) were treated as quality control for geochronology (Jackson et al., 2004; Sláma et al., 2008). Raw data reduction was performed off-line with the ICPMSDataCal software (Liu et al., 2010).

3.2 Whole-rock major and trace elements

Whole rock chemistry was determined at Nanjing FocuMS Technology Co. Ltd. Major oxides were measured using an Axios PW4400 X-ray fluorescence spectrometer (XRF) on fused glass beads. The analyses were monitored by international standard references AGV-1, BCR-2, and BHVO-1 with analytical errors of <2%. Trace element analysis were carried out with a Agilent Technologies 7700x quadrupole ICP-MS (Hachioji, Tokyo, Japan). Geochemical reference materials of USGS: basalt (BIR-1, BCR-2, BHVO-2), andesite (AVG-2), rhyolite (RGM-2), and granodiorite (GSP-2), were treated as quality control. Deviations were better than ±10% for the elements with contents lower than 10 ppm and better than ±5% for the elements with contents exceeding 50 ppm.

3.3 Whole-rock Nd isotopes

Nd isotope analyses were carried out at Nanjing FocuMS Technology Co. Ltd. Detailed analytical procedures are described by Pu et al. (2005). Diluted solution (50 ppb Nd) was introduced into a Nu

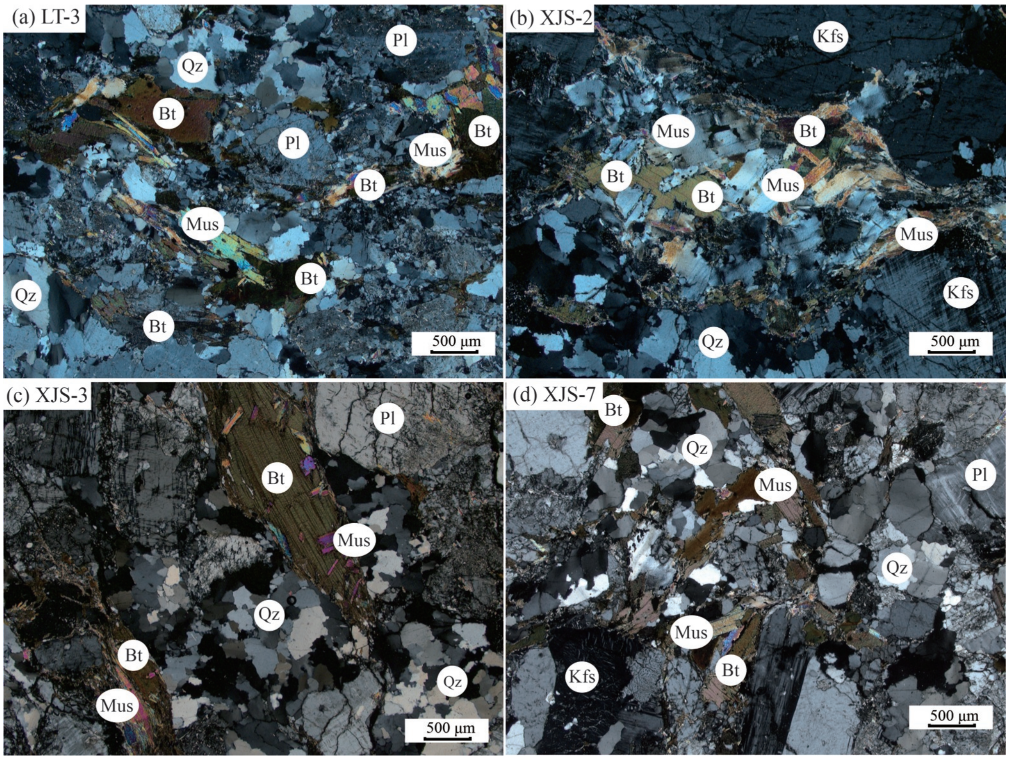

Fig. 3. Photomicrographs (under crossed polar) of the Early Jurassic Longtang (a) and Menglong (b–d) granites.
Bt–biotite; Mus–muscovite; Pl–plagioclase; Kfs–K-feldspar; Qz–quartz.

Instruments Nu Plasma II MC-ICP-MS (Wrexham, Wales, UK) through a Teledyne Cetac Technologies Aridus II desolvating nebulizer system (Omaha, Nebraska, USA). Raw data of Nd isotopic ratios were internally corrected for mass fractionation by normalizing to $^{146}Nd/^{144}Nd$ = 0.7219 with an exponential law. International isotopic standard JNdi-1 was periodically analyzed to correct instrumental drift. Geochemical reference materials of USGS (BCR-2, BHVO-2, and AVG-2) were treated as quality control. Their Nd isotopic results (BCR-2, $^{143}Nd/^{144}Nd$ = 0.512629 ± 3; BHVO-2, $^{143}Nd/^{144}Nd$ = 0.512987 ± 2; AVG-2, $^{143}Nd/^{144}Nd$ = 0.512794 ± 3) agreed with previous publications within analytical uncertainty (Weis et al., 2006, 2007).

3.4 Hf isotopes of zircon

Zircon hafnium isotopic ratios were conducted with a LA-MC-ICP-MS at Nanjing FocuMS Technology Co. Ltd., an Australian Scientific Instruments RESOlution LR laser-ablation system (Canberra, Australian), and a Nu Instruments Nu Plasma II MC-ICP-MS (Wrexham, Wales, UK) were combined for the experiments. The 193 nm ArF excimer laser was focused on zircon surfaces with a fluence of 3.5 J/cm^2. Each acquisition incorporated 20 s background (gas blank), followed by a spot diameter of 50 μm at a 9 Hz repetition rate for 40 s. Standard zircons (including GJ-1, 91500, Plešovice, Mud Tank, and Penglai) were treated as quality control every five unknown samples.

4 Results

4.1 LA-ICP-MS zircon U-Pb geochronology

LA-ICP-MS zircon U-Pb geochronology results of two samples are summarized in Supp. Table 1 and illustrated in Fig. 4. All the zircons show regular oscillatory magmatic zoning with sizes mostly between 100 and 150 μm (Fig. 4) and Th/U ratios ranging from 0.17 to 1.13 (Supp. Table 1). Fourteen analyses for sample LT-2 (Longtang granite) plot in a group on the concordia curve and yield a weighted mean $^{206}Pb/^{238}U$ age of 198.73 ± 0.72 Ma (MSWD = 0.017) (Fig. 4a). Twelve analyses for sample ML-4 (Menglong granite) plot in a group on the concordia curve and yield a weighted mean $^{206}Pb/^{238}U$ age of 199.53 ± 0.74 Ma (MSWD = 0.036) (Fig. 4b). These ages are interpreted as the crystallization ages of the granites. The LA-ICP-MS zircon U-Pb ages obtained in this work indicate that the two granites were both emplaced in the Early Jurassic (ca. 199 Ma).

4.2 Whole-rock major and trace elements

All the granitic samples have high SiO_2 contents of 69.7–75.1 wt% (Supp. Table 2). They are mainly strongly peraluminous, with alumina saturation index ASI [= molar $Al_2O_3/(CaO + Na_2O + K_2O)$] values from 1.06 to 1.46 (Fig. 5c). These rocks have high K_2O contents, with the data plotting in the fields of the shoshonitic series to the high-K calc-alkaline series (Fig. 5b). They have similar $Mg^{\#}$ [atomic $Mg/(Mg + Fe^T)$] (0.29–0.42) to experimental partial melts of metasedimentary rocks under continental pressure-temperature (P-T) conditions (Fig. 5d). These granites are enriched in light rare earth elements (LREEs) relative to heavy rare earth elements (HREEs), with moderately negative Eu anomalies and flat HREEs patterns (Fig. 6a, c). They are depleted in high field strength elements (HFSE), showing notable negative Ta-Nb and Ti anomalies (Fig. 6b, d).

4.3 Whole-rock Nd isotopes

Whole-rock Nd isotopes for the studied granitic samples are given in Supp. Table 3 and illustrated in Fig. 7. The Longtang granite exhibits Nd isotopic compositions with $\varepsilon_{Nd}(t)$ ranging from −11.8 to −12.4. The Menglong granite has similar $\varepsilon_{Nd}(t)$ values of −9.0 to −12.3. Two-stage model ages (T_{DM2}) are calculated by assuming a mean $^{147}Sm/^{144}Nd$ value of 0.118 for an average continental crust composition. As a result, both granites have Paleoproterozoic T_{DM2} ages (1.71–1.98 Ga; Supp. Table 3).

4.4 Hf isotopes of zircon

In-situ Hf isotope analyses were carried out on zircons at the same spots used for the LA-ICP-MS zircon U-Pb geochronology. The results are given in Supp. Table 1 and illustrated in Fig. 7. The Longtang

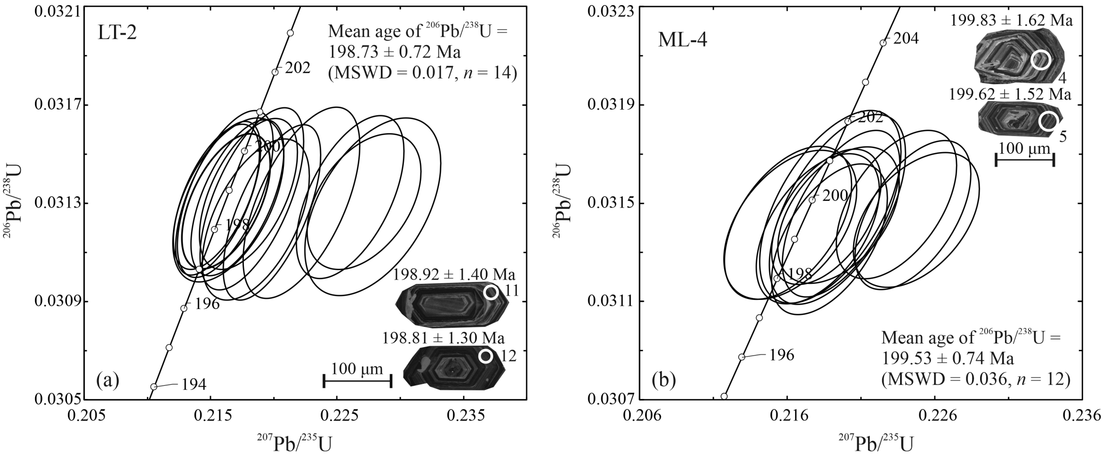

Fig. 4. Typical CL images of zircons and Concordia curves for the LA-ICP-MS zircon U-Pb geochronology of the Longtang (a) and Menglong (b) granites.

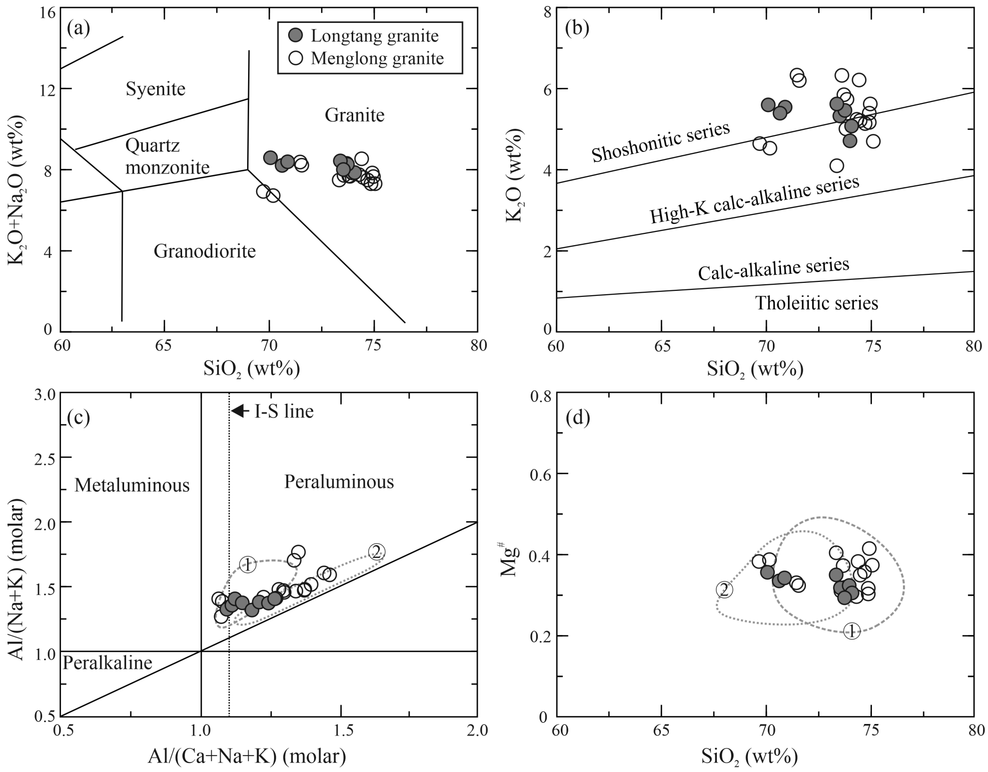

Fig. 5. (a) Total alkali-silica diagram (Middlemost, 1994); (b) SiO_2 vs. K_2O (Peccerillo and Taylor, 1976); (c) A/NK vs. A/CNK (Shand, 1943); (d) SiO_2 vs. $Mg^{\#}$ diagram for the Longtang and Menglong granites.

In (c) and (d), the fields of some experimental melts are also shown: vapor-absent partial melts (1) of a two-mica schist (plagioclase-poor natural metapelitic rock) at 7–13 kbar, 825°C–1075°C (Patiño Douce and Johnston, 1991); (2) of a biotite gneiss (plagioclase-rich synthetic metapsammitic rock) at 3–15 kbar, 875°C–1000°C (Patiño Douce and Beard, 1995).

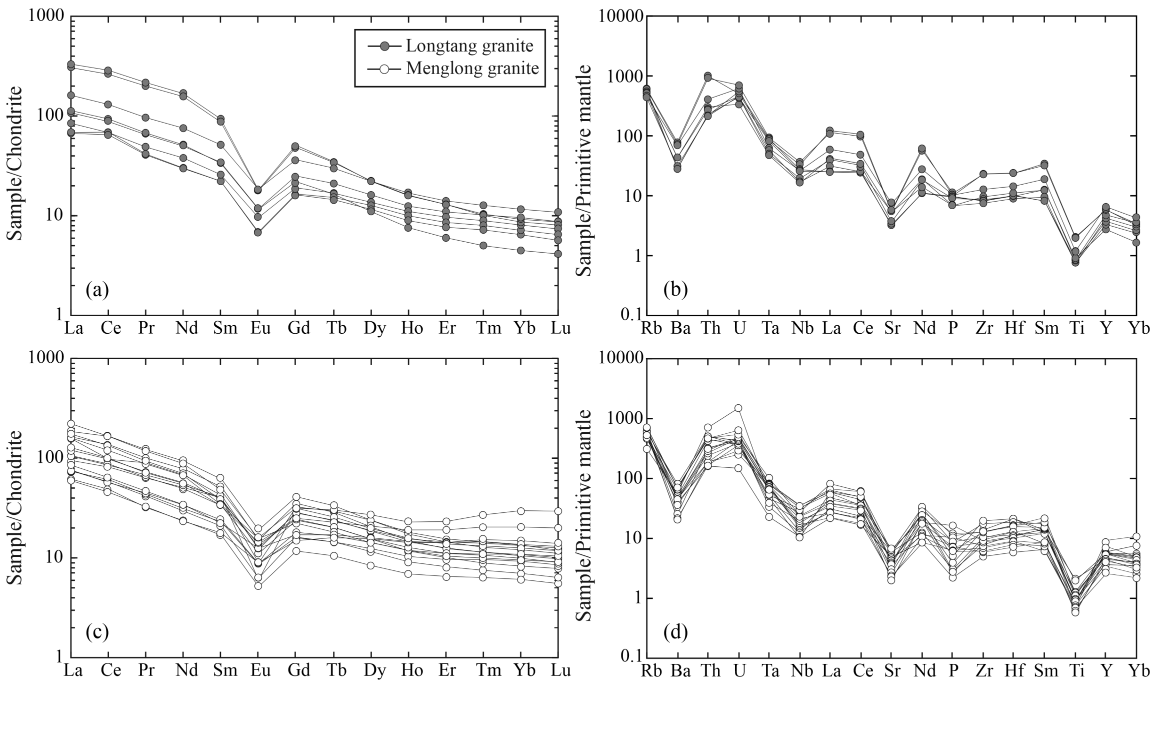

Fig. 6. Chondrite-normalized REE patterns (a, c) and primitive mantle-normalized trace element patterns (b, d) of the Longtang and Menglong granites.

The normalized values are from Sun and McDonough (1989).

granite (LT-2) has negative initial ε_{Hf} (age corrected using the U-Pb ages for individual grains) values, ranging from −6.8 to −11.8, with a weighted mean of −9.1. The Menglong granite (ML-4) has negative initial ε_{Hf} (age corrected using U-Pb ages for individual grains) values ranging from −7.2 to −8.9, with a weighted mean of −8.0. All the zircons give Paleoproterozoic two-stage model ages (T_{DM2}) (1.66–1.97 Ga). All the zircon $\varepsilon_{Hf}(t)$ values are coupled with their whole-rock $\varepsilon_{Nd}(t)$ values, and plot along the mantle array (ε_{Hf} = 1.33ε_{Nd} + 3.19; Vervoort et al., 1999; Fig. 7).

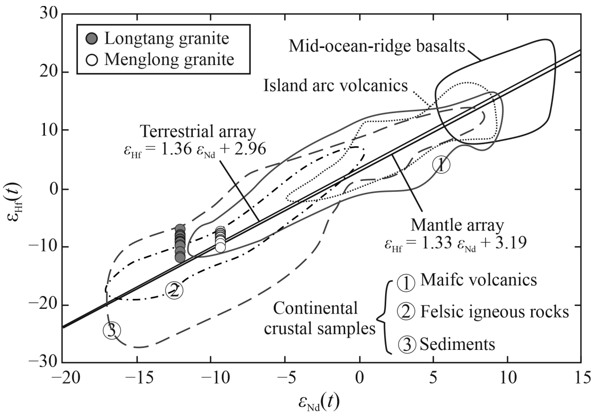

Fig. 7. Zircon $\varepsilon_{Hf}(t)$ vs. whole-rock $\varepsilon_{Nd}(t)$ (modified after Vervoort et al., 1999).

5 Discussion

5.1 Petrogenesis of the granites

The Longtang and Menglong two-mica granites contain muscovite, which is highly aluminous (Fig. 3). They are dominated by strongly peraluminous compositions, with high ASI values ranging from 1.06 to 1.46 (mostly > 1.1; Fig. 5c). All samples have high K_2O/Na_2O ratios (1.20–4.59). A negative correlation between P_2O_5 and SiO_2 is absent (Fig. 8a). Their low HFSE contents (Zr + Nb + Ce + Yb < 350 ppm) that are in contrast to A-type granites (Fig. 9a). These petrologic and geochemical features reveal that the Longtang and Menglong granites belong to S-type granites (Chappell and White, 1974; Chappell, 1999; Clemens, 2018).

Cawthorn and Brown (1976) suggested that peraluminous granites could be generated by fractional crystallization (FC) of metaluminous magmas in closed systems, accompanied by fractionation of amphibole and clinopyroxene. However, the coeval granites in the Tengchong terrane consist of peraluminous granite instead of metaluminous rocks (e.g., the Mangzhangxiang granite, Cao et al., 2019). With increasing SiO_2 contents, the lack of the increasing La/Yb ratios, decreasing Dy/Yb ratios (Fig. 10a, b), and concave REE patterns (Fig. 6a, c) also indicate insignificant fractionation of amphibole. They thus seem unlikely to be derived from FC of amphibole and clinopyroxene from metaluminous magmas. Alternatively, peraluminous granitic melts may be produced by fractionation of a mafic metaluminous magma (e.g., Zen, 1986). However, the Early Jurassic

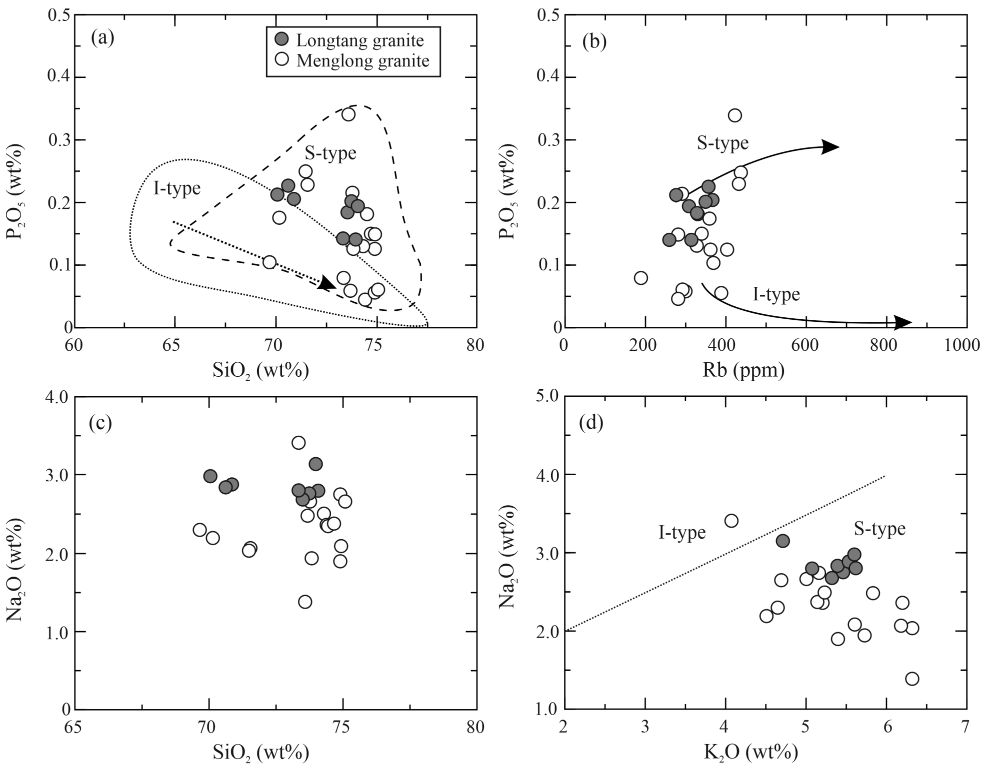

Fig. 8. (a) SiO_2 vs. P_2O_5, (b) Rb vs. P_2O_5, (c) SiO_2 vs. Na_2O, and (d) K_2O vs. Na_2O (Hine et al., 1978) plots for the Longtang and Menglong granites.
(a) and (b) modified after Chappell (1999).

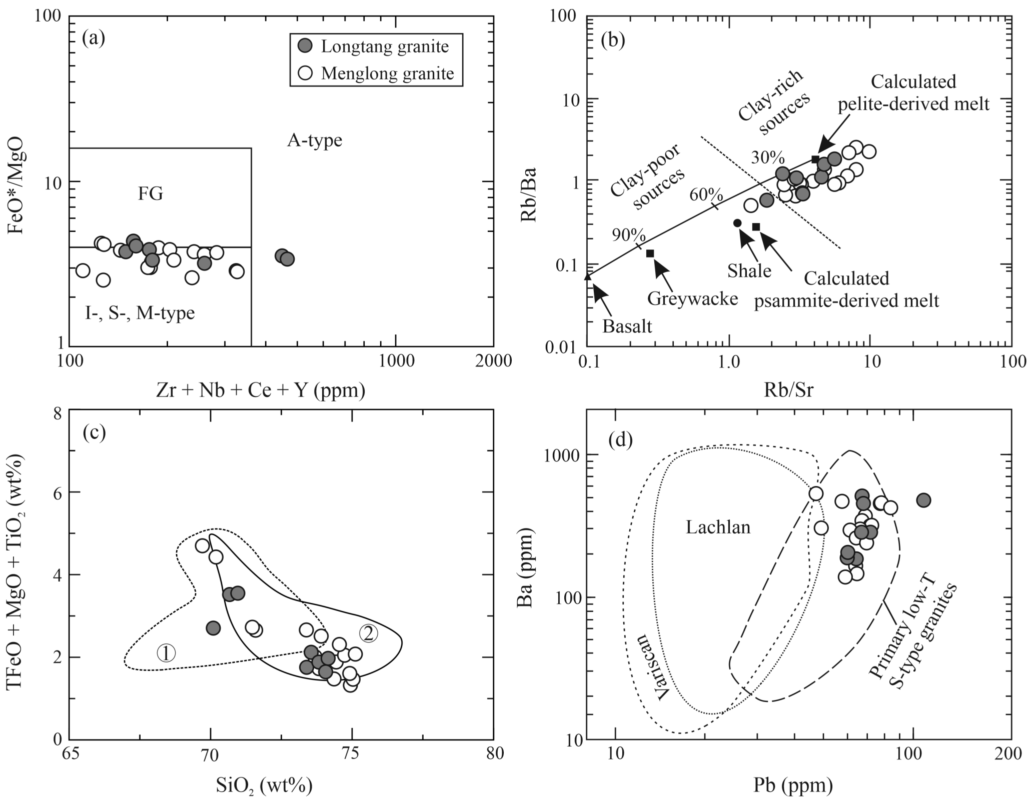

Fig. 9. (a) Zr + Nb + Ce + Y vs. FeO*/MgO (Eby, 1990), (b) Rb/Sr vs. Rb/Ba (Sylvester 1998), (c) SiO_2 vs. TFeO + MgO + TiO_2, (d) Pb vs. Ba diagrams for the Longtang and Menglong granites.
In (c), the fields of some experimental melts are also shown and the data sources are same as in Fig. 5. In (d), the fields of Lachlan, Variscan, and primary low temperature S-type granites are also shown (data are from Finger and Schiller, 2012).

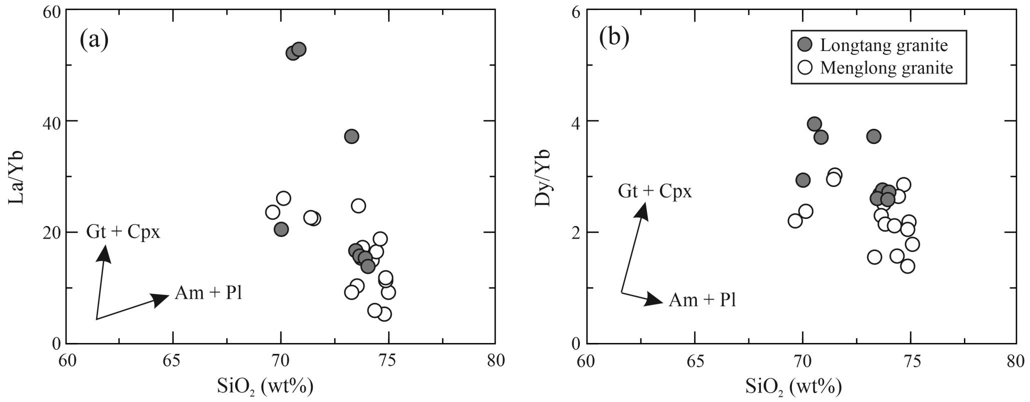

Fig. 10. (a) SiO_2 vs. La/Yb and (b) SiO_2 vs. Dy/Yb diagrams for the Longtang and Menglong granites.

Longtang and Menglong two-mica granites (ca. 199 Ma) have Nd isotopic compositions ($\varepsilon_{Nd}(t)$ values of −9.0 to −12.4) that are distinct from those of the Late Triassic (ca. 205 Ma) Yingjiang metaluminous metagabbros ($\varepsilon_{Nd}(t)$ values of −3.4 to −4.0, Zhu et al., 2018) also in the Tengchong terrane (Fig. 11a). Jiang and Zhu (2017) further suggest that extreme differentiation of plagioclase during the evolution of granitic magmas can yield strongly peraluminous magmas. But the constant Na_2O contents with increasing SiO_2 contents argue against the removal of plagioclase (Fig. 8c).

The consensus view is that strongly peraluminous granites are easy to be produced by partial melting of metasedimentary rocks (e.g., Barbarin, 1996; Sylvester, 1998; Jiang et al., 2011; Jiang and Zhu, 2017; Zhu et al., 2017; Tian et al., 2019; Yang et al., 2020; Yin et al., 2020; Zhang et al., 2020; Liu et al., 2021). The genetic model is supported by the initial Nd-Hf isotopic component of the Longtang and Menglong two-mica granites, which plot in the field of continental sediments (Fig. 7). They show evolved Nd-Hf isotopic compositions (Fig. 7), suggesting an ancient crustal source for their origin. Experimental studies demonstrate that partial melts of metasedimentary rocks (both metagreywackes and metapelites) are

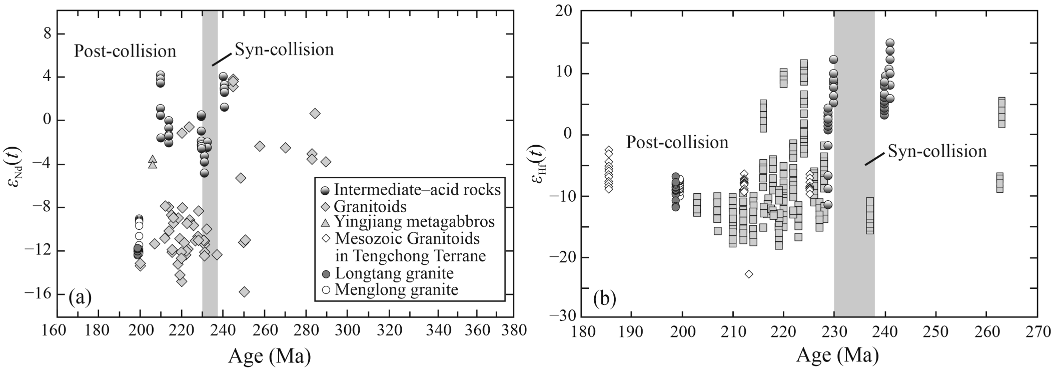

Fig. 11. (a) Whole-rock $\varepsilon_{Nd}(t)$ vs. age and (b) zircon $\varepsilon_{Hf}(t)$ vs. age for the Longtang and Menglong granites.
In (a) and (b), the data of intermediate-acidic rocks and granitoids are from Wang et al. (2018) and reference therein. Also shown are ca. 205 Ma Yingjiang metagabbros (Zhu et al., 2018) and Mesozoic granitoids of the Tengchong terrane (Cao et al., 2019).

dominated by strongly peraluminous compositions (ASI > 1.1; Patiño Douce and Johnston, 1991; Patiño Douce and Beard, 1995). All the samples exhibit similar $Mg^{\#}$ and $TFeO + MgO + TiO_2$ values to experimental melts of metasedimentary rocks (Figs. 5d, 9c). Furthermore, the relatively low FeO^{*}/MgO ratios (2.5 to 4.3) plot in the field of unfractionated granites (Fig. 9a), suggesting that these granitic samples can represent the components of the primary crustal partial melts. The relatively high Rb/Sr and Rb/Ba ratios (Fig. 9b) further indicate their derivation from a metapelitic source. At lower temperatures in the range of 700°C to 750°C, the fluid-absent melting is controlled by muscovite breakdown with the reaction of muscovite (Ms) + quartz (Qtz) + plagioclase (Pl) = melt + sillimanite (Sil) ± K-feldspar (Kfs) or the reaction of Ms + biotite (Bt) + Qtz + Pl = melt + Grt + Sil ± Kfs (Vielzeuf and Holloway, 1988). In contrast, at higher temperatures ranging from ~800°C to 900°C, fluid-absent melting is triggered by biotite breakdown, which is involved in the reactions of Bt + Sil + Qtz + Pl = melt + cordierite + Grt ± Kfs and Bt + Qtz + Pl = melt + Opx ± Grt ± Kfs (Le Breton and Thompson, 1988; Vielzeuf and Holloway, 1988; Vielzeuf and Montel, 1994). Because Pb is more compatible in muscovite than in biotite, in contrast to high -*T* melting for biotite breakdown, low-*T* melting of muscovite-rich metasedimentary sources can release large amounts of Pb (Finger and Schiller, 2012). Thus, the high Pb contents of the two granites support a low-temperature melting process (Fig. 9d). The relatively flat HREE patterns (Fig. 6a, c) reveal that garnet was not a residual phase after partial melting (Lin et al., 2018). The markedly negative Eu and Sr anomalies support the presence of plagioclase as a residual mineral phase (Fig. 6a, c). These geochemical signatures imply that the partial melting occurred at <10 kbar (corresponding to a normal crustal depth of <33 km) (Vielzeuf and Holloway, 1988; Jiang et al., 2010). In summary, we consider that these two-mica granites likely formed by muscovite-dehydration melting of a metapelitic source at lower temperatures in the range of 700°C to 750°C at a normal crustal depth.

5.2 Tectonic setting

Two Early Jurassic granites in the Tengchong terrane were previously reported: the Lianghe weakly peraluminous biotite granite (ca. 195.5 Ma; Zhu et al., 2018) and the Manzhangxiang S-type granite (ca. 185.6 Ma; Cao et al., 2019). They were suggested to be derived from certain crustal sources. The Lianghe granite presumably originated from melting of a metasedimentary source mainly dominated by metagreywacke and/or psammite (Zhu et al., 2018). The Manzhangxiang granite was suggested to be generated by partial melting of Paleoproterozoic–Mesoproterozoic Gaoligong crust crustal rocks (Cao et al., 2019). But their tectonic settings remains controversial. Zhu et al. (2018) considered that the Tengchong terrane and the Lhasa terrane have experienced similar tectonomagmatic history since the Early Paleozoic. The Early Jurassic crustal-derived granitoid magmatism was thought to be generated by the Late Triassic (after ca. 235 Ma) collision between the Lhasa–Tengchong terrane and the northern margin of the Australian continent. In contrast, Cao et al. (2019) suggested that the Tengchong terrane should be taken as the southeastern extension of the Qiangtang terrane. Similar to the Early Jurassic magmatic rocks in southern Qiangtang terrane, the Early Jurassic granite in the Tengchong terrane was derived by the partial melting of crust that was triggered by the initial deep subduction of the Meso-Tethys Ocean. Furthermore, Wang et al. (2018) proposed that final closure of the Paleo-Tethys Ocean began in the Triassic Ladinian Stage (~237 Ma). The 237–230 Ma granitic rocks along the Paleo-Tethys suture are interpreted as the product of syn-collisional magmatism, whereas the 230–200 Ma granitic rocks are considered as products of post-collisional magmatism. The East Paleotethyan orogen terminated at ca. 200 Ma in Southeast Asia.

Recent study of the Myanmar ophiolites suggests that the Myitkyina ophiolite (ca. 171–166 Ma; Yang et al., 2012; Liu et al., 2016) is the southern extension of the Bangong–Nujiang suture that corresponds to the suture of the Meso-Tethys Ocean (Liu et al., 2016). It thus most likely that the suture of the Meso-Tethys Ocean is located in between the West Burma terrane and the Tengchong terrane. In this scenario, the Tengchong terrane is the southern extension of the South Qiangtang terrane instead of the Lhasa terrane (Fang et al., 2018; Cao et al., 2019). Previous studies also suggested that the Tengchong terrane, in the northern part of the Sibumasu terrane, finally collided with the Simao-Indochina terrane (Metcalfe, 2013; Wang et al., 2018). We therefore rule out the possibility that the Early Jurassic granitoids in the Tengchong terrane were associated with the collision between the Lhasa-Tengchong terrane and the northern margin of the Australian continent. A small quantity of Early Jurassic granites (ca. 199–186 Ma) occurred in the Tengchong terrane ahead of the extensive Early Cretaceous granites emplaced (ca. 140 Ma to 110 Ma, Cao et al., 2019). In contrast, the granitoids in the Qiangtang terrane mainly formed from ca. 185 Ma to 150 Ma (Liu et al., 2017). It is difficult to imagine a prolonged period of quiescent magmatism (ca. 186–140 Ma) in the Tengchong terrane if subduction was ongoing. Furthermore, the petrogenesis of the Longtang and Menglong two-mica granites suggest that they were derived from the normal crustal depth (<33 km) instead of thickened crust. It is more reasonable to interpret the Early Jurassic magmatism in the Tengchong terrane as the post-collisional response of the Paleo-Tethyan regime. The East Paleotethyan orogen thus finally terminated at ca. 186 Ma in the Tengchong terrane.

6 Conclusions

(1) The Early Jurassic Longtang and Menglong two-mica granites in the Tengchong terrane are likely to have been formed by muscovite-dehydration melting of a metapelitic source at lower temperatures in the range of 700°C to 750°C.

(2) The Early Jurassic granites in the Tengchong terrane were most likely formed in the post-collisional tectonic setting following the closure of the Paleo-Tethys Ocean.

Acknowledgments

This work was financially supported by the National Natural Science Foundation of China (Grant No. 41903032), Science (Engineering) Research Project of Yunnan University (Grant No. 2017YDQN08), and Applied Basic Research Programs of Science and Technology Department of Yunnan Province (Grant No. 2018FD009). We are grateful to two anonymous reviewers for their thoughtful reviews and constructive comments.

Manuscript received Jan. 02, 2020
accepted Jun. 08, 2021
associate EIC: FEI Hongcai
edited by GUO Xianqing

Supplementary data to this article can be found online at http://doi.org/10.1111/1755-6724.14925.

References

Barbarin, B., 1996. Genesis of the two main types of peraluminous granitoids. Geology, 24(4): 295–298.

BGMRY, 1983. Geological Map Sheet Tengchong. Bureau of Geology and Mineral Resources of Yunnan Province, scale 1:200000 (in Chinese).

Cai, F.L., Ding, L., Yao, W., Laskowski, A.K., Xu, Q., Zhang, J.E., and Sein, K., 2017. Provenance and tectonic evolution of Lower Paleozoic–Upper Mesozoic strata from Sibumasu terrane, Myanmar. Gondwana Research, 41: 325–336.

Cao, H.W., Zhang, S.T., Lin, J.Z., Zheng, L., Wu, J.D., and Li, D., 2014. Geology, geochemistry and geochronology of the Jiaojiguanliangzi Fe-polymetallic deposit, Tengchong County, Western Yunnan (China): Regional tectonic implications. Journal of Asian Earth Sciences, 81: 142–152.

Cao, H.W., Zou, H., Zhang, Y.H., Zhang, S.T., Zheng, L., Zhang, L.K., Tang, L., and Pei, Q.M., 2016. Late Cretaceous magmatism and related metallogeny in the Tengchong area: Evidence from geochronological, isotopic and geochemical data from the Xiaolonghe Sn deposit, western Yunnan, China. Ore Geology Reviews, 78: 196–212.

Cao, H.W., Zhang, Y.H., Pei, Q.M., Zhang, R.Q., Tang, L., Lin, B., and Cai, G.J., 2017. U-Pb dating of zircon and cassiterite from the Early Cretaceous Jiaojiguan iron-tin polymetallic deposit, implications for magmatism and metallogeny of the Tengchong area, western Yunnan, China. International Geology Review, 59(2): 234–258.

Cao, H.W., Zhang, Y.H., Santosh, M., Zhang, S.T., Tang, L., Pei, Q.M., and Yang, Q.Y., 2018. Mineralogy, zircon U-Pb-Hf isotopes, and whole-rock geochemistry of Late Cretaceous–Eocene granites from the Tengchong terrane, western Yunnan, China: Record of the closure of the Neo-Tethyan Ocean. Geological Journal, 53(4): 1423–1441.

Cao, H.W., Zhang, Y.H., Tang, L., Hollis, Steven. P., Zhang, S.T., Pei, Q.M., Yang C., and Zhu, X.S., 2019. Geochemistry, zircon U-Pb geochronology and Hf isotopes of Jurassic–Cretaceous granites in the Tengchong terrane, SW China: Implications for the Mesozoic tectono-magmatic evolution of the Eastern Tethyan Tectonic Domain. International Geology Review, 61(3): 257–279.

Cawthorn, R.G., and Brown, P.A., 1976. A model for the formation and crystallization of corundum-normative calc-alkaline magmas through amphibole fractionation. The Journal of Geology, 84(4): 467–476.

Chappell, B.W., 1999. Aluminium saturation in I- and S-type granites and the characterization of fractionated haplogranites. Lithos, 46(3): 535–551.

Chappell, B.W., and White, A.J.R., 1974. Two contrasting granite types. Pacific Geology, 8(2): 173–174.

Chen, X.C., Hu, R.Z., Bi, X.W., Zhong, H., Lan, J.B., Zhao, C.H., and Zhu, J.J., 2015. Petrogenesis of metaluminous A-type granitoids in the Tengchong–Lianghe tin belt of southwestern China: Evidences from zircon U-Pb ages and Hf -O isotopes, and whole-rock Sr-Nd isotopes. Lithos, 212–215: 93–110.

Clemens, J.D., 2018. Granitic magmas with I-type affinities, from mainly metasedimentary sources: The Harcourt batholith of southeastern Australia. Contributions to Mineralogy and Petrology, 173(11): 1–20.

Cong, F., Lin, S.L., Tang, H.F., Xie, T., Li, Z.H., Zou, G.F., Peng, Z.M., and Liang, T., 2010. Trace elements and Hf isotope compositions and U-Pb age of igneous zircons from the Triassic Granite in Lianghe, Western Yunnan. Acta Geological Sinica, 84(8): 1155–1164 (in Chinese with English abstract).

Eby, G.N., 1990. The A-type granitoids: A review of their occurrence and chemical characteristics and speculations on their petrogenesis. Lithos, 26: 115–134.

Fang, Y., Zhang, Y. H., Zhang, S.T., Cao, H.W., Zou, H., and Dong, J.H., 2018. Early Cretaceous I-type granites in the Tengchong terrane: New constraints on the late Mesozoic tectonic evolution of southwestern China. Geoscience Frontiers, 9(2): 459–470.

Feng, Q.L., 2002. Stratigraphy of volcanic rocks in the Changning–Menglian belt in Southwestern Yunnan, China. Journal of Asian Earth Sciences, 20(6): 657–664.

Finger, F., and Schiller, D., 2012. Lead contents of S-type granites and their petrogenetic significance. Contributions to Mineralogy and Petrology, 164(5): 747–755.

Hennig, D., Lehmann, B., Frei, D., Belyatsky, B., Zhao, X.F., Cabral, A.R., Zeng, P.S., Zhou, M.F., and Schmidt, K., 2009. Early Permian seafloor to continental arc magmatism in the eastern Paleo-Tethys: U-Pb age and Nd-Sr isotope data from the southern Lancangjiang zone, Yunnan, China. Lithos, 113:

408–422.

Hine, R., Williams, I.S., Chappell, B.W., and White, J.R., 1978. Contrasts between I- and S-type granitoids of the Kosciusko Batholith. Journal of the Geological Society of Australia, 25(3–4): 219–234.

Huang, Z.Y., Qi, X.X., Tang, G.Z., Liu, J.K., Zhu, L.H., Hu, Z.C., Zhao, Y.H., and Zhang, C., 2013. The identification of early Indosinian tectonic movement in Tengchong block, western Yunnan: Evidence of zircon U-Pb dating and Lu-Hf isotope for Nabang diorite. Geology in China, 40(3): 730–741 (in Chinese with English abstract).

Jackson, S.E., Pearson, N.J., Griffin, W.L., and Belousova, E.A., 2004. The application of laser ablation-inductively coupled plasma-mass spectrometry to in situ U-Pb zircon geochronology. Chemical Geology, 211(1–2): 47–69.

Jiang, Y.H., Jin, G.D., Liao, S.Y., Zhou, Q., and Zhao, P., 2010. Geochemical and Sr-Nd-Hf isotopic constraints on the origin of Late Triassic granitoids from the Qinling orogen, central China: Implications for a continental arc to continent-continent collision. Lithos, 117: 183–197.

Jiang, Y.H., Zhao, P., Zhou, Q., Liao, S.Y., and Jin, G.D., 2011. Petrogenesis and tectonic implications of Early Cretaceous S- and A-type granites in the northwest of the Gan-Hang rift, SE China. Lithos, 121: 55–73.

Jiang, Y.H., and Zhu, S.Q., 2017. Petrogenesis of the Late Jurassic peraluminous biotite granites and muscovite-bearing granites in SE China: Geochronological, elemental and Sr-Nd-O-Hf isotopic constraints. Contributions to Mineralogy and Petrology, 172(11–12): 101.

Le Breton, N., and Thompson, A.B., 1988. Fluid-absent (dehydration) melting of biotite in metapelites in the early stages of crustal anatexis. Contributions to Mineralogy and Petrology, 99(2): 226–237.

Li, D.P., Chen, Y.L., Hou, K.J., and Luo, Z.H., 2016. Origin and evolution of the Tengchong block, southeastern margin of the Tibetan Plateau: Zircon U-Pb and Lu-Hf isotopic evidence from the (meta-) sedimentary rocks and intrusions. Tectonophysics, 687: 245–256.

Lin, L., Qiu, J.S., Wang, R.Q., Hong, Y.F., and Xu, H., 2018. Magma Mixing in Oligocene Granites from Nyemo, Tibet: Implications for Petrogenesis and Continental Crust Accretion. Acta Geologica Sinica, 92(12): 2388–2409 (in Chinese with English abstract).

Liu, C.Z., Chung, S.L., Wu, F.Y., Zhang, C., Xu, Y., Wang, J.G., Chen, Y., and Guo, S., 2016. Tethyan suturing in Southeast Asia: Zircon U-Pb and Hf-O isotopic constraints from Myanmar ophiolites. Geology, 44(4): 311–314.

Liu, D.L., Shi, R.D, Ding, L., Huang, Q.S., Zhang, X.R., Yue, Y.H., and Zhang, L.Y., 2017. Zircon U-Pb age and Hf isotopic compositions of Mesozoic granitoids in southern Qiangtang, Tibet: Implications for the subduction of the Bangong–Nujiang Tethyan Ocean. Gondwana Research, 41: 157–172.

Liu, Y.S., Hu, Z.C., Zong, K.Q., Gao, C.G., Gao, S., Xu, J., and Chen, H.H., 2010.Reappraisement and refinement of zircon U-Pb isotope and trace element analyses by LA-ICP-MS. Chinese Science Bulletin, 55(15): 1535–1546.

Liu, C.F., Zhou, Z.G., Wang, G.S., Wu, C., Li, H.Y., Ma, S.W., 2021. Carboniferous ridge subduction in the Xingmeng Orogenic Belt: Constraints from geochronological, geochemical, and Sr-Nd-Hf isotopic analysis of strongly peraluminous granites and gabbro-diorites in the Xilinhot micro-continent. Geoscience Frontiers, 12(3): 101103.

Metcalfe, I., 2011a. Palaeozoic–Mesozoic history of SE Asia. In: Hall, R., Cottam, M., and Wilson, M. (eds.), The SE Asian Gateway: History and Tectonics of Australia–Asia Collision. Geological Society of London Special Publications, 355: 7–35.

Metcalfe, I., 2011b. Tectonic framework and Phanerozoic evolution of Sundaland. Gondwana Research, 19(1): 3–21.

Metcalfe, I., 2013. Gondwana dispersion and Asian accretion: Tectonic and palaeogeographic evolution of eastern Tethys. Journal of Asian Earth Sciences, 66: 1–33.

Metcalfe, I., Henderson, C. M., and Wakita, K., 2017. Lower Permian conodonts from Palaeo-Tethys ocean plate stratigraphy in the Chiang Mai-Chiang Rai suture zone, northern Thailand. Gondwana Research, 44: 54–66.

Middlemost, E.A., 1994. Naming materials in the magma/igneous rock system. Earth-Science Reviews, 37(3–4): 215–224.

Patiño Douce, A.E., and Beard, J.S., 1995. Dehydration-melting of biotite gneiss and quartz amphibolite from 3 to 15 kbar. Journal of Petrology, 36(3): 707–738.

Patiño Douce, A.E., and Johnston, A.D., 1991. Phase equilibria and melt productivity in the pelitic system: Implications for the origin of peraluminous granitoids and aluminous granulites: Contributions to Mineralogy and Petrology, 107: 202–218.

Pearce, J., 1996. Sources and settings of granitic rocks. Episodes, 19: 120–125.

Peccerillo, A., and Taylor, S.R., 1976. Geochemistry of Eocene calc-alkaline volcanic rocks from the Kastamonu area, northern Turkey. Contributions to mineralogy and petrology, 58(1): 63–81.

Pitcher, W.S., 1997. The nature and origin of granite. Springer Science & Business Media.

Pu, W., Gao, J.F., Zhao, K.D., Ling, H.F., and Jiang, S.Y., 2005. Separation method of Rb-Sr, Sm-Nd using DCTA and HIBA. Journal of Nanjing University (Natural Sciences), 41(4): 445–450.

Searle, M.P., Whitehouse, M.J., Robb, L.J., Ghani, A.A., Hutchison, C.S., Sone, M., Ng, S.W.P., Roselee, M.H., Chung, S.L., and Oliver, G.J.H., 2012. Tectonic evolution of the Sibumasu-Indochina terrane collision zone in Thailand and Malaysia: Constraints from new U-Pb zircon chronology of SE Asian tin granitoids. Journal of the Geological Society, 169(4): 489–500.

Shand, S.J., 1943. Eruptive Rocks. Their Genesis Composition. Classification, and Their Relation to Ore-Deposits with a Chapter on Meteorite. John Wiley & Sons, New York.

Sláma, J., Košler, J., Condon, D.J., Crowley, J.L., Gerdes, A., Hanchar, J.M., Horstwood, M.S.A., Morris, G.A., Nasdala, L., Norberg, N., Schaltegger, U., Schoene, B., Tubrett, M.N., and Whitehouse, M.J., 2008. Plešovice zircon—A new natural reference material for U-Pb and Hf isotopic microanalysis. Chemical Geology, 249(1–2): 1–35.

Song, S.G., Niu, Y.L., Wei, C.J., Ji, J.Q., and Su, L., 2010. Metamorphism, anatexis, zircon ages and tectonic evolution of the Gongshan block in the northern Indochina continent—An eastern extension of the Lhasa Block. Lithos, 120: 327–346.

Sun, S.S., and McDonough, W.F., 1989. Chemical and isotopic systematics of oceanic basalts: Implications for mantle composition and processes. In: Sauders, A.D., and Norry, M.J. (eds.), Magmatism in the Ocean Basins. Geological Society London Special Publications, 42(1): 313–345.

Sylvester, P.J., 1998. Post-collisional strongly peraluminous granites. Lithos, 45: 29–44.

Tian, J., Zhang, Y., Teng, X.J., Liu, Y., Teng, F., Guo, S., He, P., and Wang, W.L., 2019. The determination of Late Silurian two-mica monzonitic granite pluton in the Langshan area, Inner Mongolia and its geological implication. Acta Geologica Sinica, 93(3): 661–673 (in Chinese with English abstract).

Vervoort, J., Patchett, P.J., Blichert-Toft, J., and Albarede, F., 1999. Relationships between Lu-Hf and Sm-Nd isotopic systems in the global sedimentary system. Earth and Planetary Science Letters, 168(1–2): 79–99.

Vielzeuf, D., and Holloway, J.R., 1988. Experimental determination of the fluid-absent melting relations in the pelitic system. Contributions to Mineralogy and Petrology, 98(3): 257–276.

Vielzeuf, D., and Montel, J.M., 1994. Partial melting of metagreywackes. Part I. Fluid-absent experiments and phase relationships. Contributions to Mineralogy and Petrology, 117(4): 375–393.

Wang, Y.J., Qian, X., Cawood, P. A., Liu, H.C., Feng, Q.L., Zhao, G.C., Zhang, Y.H., He, H.Y., and Zhang, P.Z., 2018. Closure of the East Paleotethyan Ocean and amalgamation of the Eastern Cimmerian and Southeast Asia continental fragments. Earth-Science Reviews, 186: 195–230.

Weis, D., Kieffer, B., Maerschalk, C., Barling, J., Jong, J., Williams, G.A., Hanano, D., Pretorius, W., Mattielli, N., Scoates, J.S., Goolaerts, A., Friedman, R.M., and Mahoney, J.B., 2006. High-precision isotopic characterization of USGS reference materials by TIMS and MC-ICP-MS. Geochemistry, Geophysics, Geosystems, 7(8): 1–30.

Weis, D., Kieffer, B., Hanano, D., Nobre Silva, I., Barling, J., and Pretorius, W., 2007. Hf isotope compositions of U.S. Geological Survey reference materials. Geochemistry, Geophysics, Geosystems, 8(6): 1–15.

Wiedenbeck, M., Alle, P., Corfu, F., Griffin, W.L., Meier, M., Oberli, F., Von quadt, A., Roddick, J.C., and Spiegel, W., 1995. Three natural zircon standards for U-Th-Pb, Lu-Hf, trace element and REE analyses. Geostandards Newsletter, 19 (1): 1–23.

Xie, J.C., Zhu, D.C., Dong, G.C., Zhao, Z.D., Wang, Q., and Mo, X.X., 2016. Linking the Tengchong Terrane in SW Yunnan with the Lhasa Terrane in southern Tibet through magmatic correlation. Gondwana Research, 39: 217–229.

Yang, J.S., Xu, Z.Q., Duan, X.D., Li, J., Xiong, F.H., Liu, Z., Cai, Z.H., and Li, H.Q., 2012. Discovery of a Jurassic SSZ ophiolite in the Myitkyina region of Myanmar. Acta Petrologica Sinica, 28(6): 1710–1730 (in Chinese with English abstract).

Yang, C.D., Ding, J.G., Yang, F.Q., Li, Q., and Zhang, Z.L., 2020.Geochemistry and its geological significance of the Ordovician granite from the Bieyesamasi deposit, Altay, Xinjiang. Geological Review, 66(6): 1499–1514 (in Chinese).

Yin, Q.Q., Xiang, X.K., Yu, Z.D., Yang, X.F., Wang, T.C., Zhong, B., Tan, R., Liao, J.H., and Zhu, Y.S., 2020.Genesis of S-type granites in the Pengshan Sn-polymetallic ore field, northern Jiangxi Province and its implications. Acta Geologica Sinica (English Edition), 94(6): 1860–1873.

Zen, E.A., 1986. Aluminum enrichment in silicate melts by fractional crystallization: Some mineralogic and petrographic constraints. Journal of Petrology, 27(5): 1095–1117.

Zhang, H.D., Liu, J.C., Yang, J.K., Ge, J.K., Wang, J.Y., and Li, Z., 2020. Testing final closure time of the Paleo-Asian Ocean along the Solonker suture by a transition of compressional and extensional setting. Geoscience Frontiers, 11(6): 1935–1951.

Zhong, D.L., 1998. The Paleotethys orogenic belt in west of Sichuan and Yunnan. Science Publishing House Beijing, 1–230 (in Chinese).

Zhu, D.C., Wang, Q., Zhao, Z.D., Chung, S.L., Pa, C., Niu, Y.L., Liu, S., Wu, F.Y., and Mo, X.X., 2015. Magmatic record of India-Asia collision. Scientific Reports, 5: 14289.

Zhu, R.Z., Lai, S.C., Qin, J.F., and Zhao, S.W., 2018. Petrogenesis of late Paleozoic-to-early Mesozoic granitoids and metagabbroic rocks of the Tengchong Block, SW China: Implications for the evolution of the eastern Paleo-Tethys. International Journal of Earth Sciences, 107(2): 431–457.

Zhu, Y., Lai, S.C., and Qin, J.F., 2017. Petrogenesis of Late Triassic two-mica granite in Guanyinqiao, Jinchuan area, Songpan orogenic belt, and its geological significance. Geological Review, 63(6): 1465–1478 (in Chinese with English abstract).

Zou, G.F., Lin, S.L., Li, Z.H., Cong, F., and Xie, T., 2011. Geochronology and geochemistry of the Longtang granite in the Lianghe area, Western Yunnan and its tectonic implications. Geotectonica et Metallogenia, 35(3): 439–451 (in Chinese with English abstract).

About the first author

WANG Guochang, male, born in 1988 in Lijiang, Yunnan Province; Ph.D.; graduated from Kunming University of Science and Technology and Nanjing University; research assistant at the Institute of Palaeontology, Yunnan University; He is now interested in the study on petrogenesis of the granitoids; E-mail: gcwang@ynu.edu.cn.

About the corresponding author

LIU Zheng, male, born in 1988 in Xinyang, Henan Province; Ph.D.; graduated from Jilin University and Nanjing University; associate professor of School of Earth Science, Yunnan University. He is now interested in the study on petrogenesis of the granitoids and MMEs, granitoids and crustal growth, and mineralization of the granitoids related deposit; E-mail: liuzheng.0311@163.com.